EEET ECOLOGICAL ENGINEERING & ENVIRONMENTAL TECHNOLOGY

Ecological Engineering & Environmental Technology, 2026, 27(5), 183–199
https://doi.org/10.12912/27197050/220214
ISSN 2719–7050, License CC-BY 4.0

Received: 2026.03.14
Accepted: 2026.04.15
Published: 2026.05.01

Integrated methodological framework for managed recharge of heterogeneous karst aquifers through deep injection wells

Gerardo Augusto Montemayor-Ahuja[1*], Ricardo Alberto Cavazos-González[1], Héctor de León-Gómez[1], Mariana Pérez-Martínez[1]

[1] Facultad de Ingeniería Civil, Universidad Autónoma de Nuevo León, Av. Universidad S/N, Cd. Universitaria, 66455 San Nicolás de los Garza, Nuevo León, México
* Corresponding author's e-mail: gmontemayoraj@uanl.edu.mx

ABSTRACT

The development of a deep injection well in a karst environment was carried out to establish an underground storage system in Galería Los Elizondo, México, aimed at mitigating drought impacts and strengthening regional water supply resilience. The research was designed as an applied study integrating topographic surveying, geological and geotechnical characterization, geophysical investigations, hydrological analysis, and hydrogeological evaluation to support the conceptual design of the recharge well. The site defined a surface catchment area of 15 × 30 m (450 m²; 0.045 ha) determined through relief and runoff assessment. Geophysical characterization using magnetotelluric and transient electromagnetic methods identified resistivities ranging from 23 to 270 Ω·m within the upper hundreds of meters, as well as zones with values on the order of approximately 1,000 Ω·m associated with lithological variations typical of karst environments. The hydrogeological assessment considered two strata with thicknesses of 20 m (K = 100 m/day) and 90 m (K = 10 m/day), parameters used to estimate the conceptual hydraulic behavior of the system. Piezometric monitoring at four points recorded average static levels of 625.167, 625.017, 620.946, and 612.897 masl (meters above sea level), with an overall mean elevation of 621.007 masl. Hydrological analysis estimated a maximum surface runoff discharge of 105 L/s and, using adopted temporal parameters (T_c = 5.00 min; T_p = 5.24 min), a total event volume of 370.41 m³ and an effective transient storage volume of 40.58 m³. Critical volumes on the order of −4.51 m³ were identified, with an estimated filling time between 15 and 45 minutes. The integrated process enabled the sequential articulation of the technical components required to structure a systematic procedure for managed recharge in heterogeneous karst aquifers under complex geological conditions.

Keywords: aquifer recharge, karst aquifer, injection well, electrical resistivity, hydrological analysis.

INTRODUCTION

The metropolitan area of Monterrey has experienced recurrent drought episodes during the last decade that have reduced the availability of surface water and intensified pressure on regional groundwater resources. Declining reservoir storage, irregular precipitation patterns, and sustained urban growth have revealed structural vulnerabilities in the regional water supply system (Neri & Magaña, 2016). Dependence on surface sources exposed to climatic variability has generated periods of critical shortage and has renewed interest in alternative strategies capable of improving water storage and long-term supply stability. Galería Los Elizondo is located within this regional context and faces similar limitations regarding water availability, regulation capacity, and storage of the resource.

Arid and semi-arid climatic conditions dominate northeastern México and restrict natural groundwater recharge. Recharge processes depend largely on short-duration precipitation events that generate rapid runoff and irregular infiltration contributions (Palma et al., 2022). Increasing domestic and urban demand has progressively reduced the margin between water

availability and water consumption. Periods of drought therefore expose the absence of mechanisms capable of storing water during periods of greater availability and regulating its use during deficit conditions. Technical alternatives supported by hydrological and hydrogeological analyses are required to address this imbalance (Cruz-Ayala and Megdal, 2020).

The geological framework of the region corresponds to a heterogeneous karst environment composed primarily of carbonate formations affected by dissolution processes. Karst aquifers are characterized by fractures, bedding planes, dissolution cavities, and preferential conduits that control groundwater circulation (Cristiano et al., 2017). The evolution of karst systems produces complex networks of interconnected voids whose spatial distribution is highly irregular. Hydraulic conductivity may vary by several orders of magnitude over short distances depending on the degree of fracturing and conduit development (Hartmann et al., 2014). Such structural heterogeneity introduces significant uncertainty in the interpretation of groundwater flow and storage capacity. Localized storage zones and hydraulic anisotropy complicate predictions of aquifer response to recharge interventions and require careful evaluation of subsurface conditions (Goldscheider et al., 2020).

Deep injection recharge has been proposed as a technical alternative capable of increasing groundwater storage under controlled conditions, particularly in structurally complex aquifers. Its application in karst environments requires detailed characterization of the receiving medium and the integration of multiple sources of information. Surface catchment areas must be defined through topographic analysis and runoff dynamics. Geological and geotechnical investigations provide information about lithology, structural continuity, and ground stability. Geophysical exploration, particularly magnetotelluric and transient electromagnetic methods, allows the identification of resistivity contrasts associated with lithological changes and structural discontinuities in the subsurface (Binley et al., 2015). These analyses provide an initial interpretation of subsurface conditions prior to drilling operations.

Galería Los Elizondo forms part of the hydrological system that supplies the metropolitan region of Monterrey, where increasing groundwater demand and limited recharge conditions have intensified the need for alternative storage strategies (Stefan and Ansems, 2018). The heterogeneous karst structure of the aquifer introduces substantial uncertainty in predicting hydraulic behavior. Fractures, dissolution features, and preferential conduits strongly influence groundwater circulation in karst aquifers, making rigorous technical evaluation necessary before implementing recharge interventions (Famiglietti, 2014).

The development of groundwater storage through deep injection therefore requires determining whether geological structure, hydrological inputs, and hydraulic characteristics of the karst aquifer allow the implementation of a technically viable recharge scheme. Such evaluation involves the analysis of topographic configuration, geological structure, geotechnical conditions, geophysical information, and hydrological behavior in order to identify suitable recharge locations and estimate aquifer response. In heterogeneous karst environments, where subsurface flow is controlled by fractures and preferential conduits, the integration of geophysical characterization with hydrological and hydrogeological analyses becomes essential to reduce uncertainty in recharge system performance.

The present research evaluates the conceptual feasibility of deep injection as an underground storage alternative in a heterogeneous karst aquifer located in Galería Los Elizondo under the hydrological conditions of the Monterrey metropolitan region (Binley et al., 2015). The study proposes an integrated methodological framework that combines topographic analysis, geophysical investigation, hydrogeological characterization, hydrological modeling, and volumetric verification of system performance under extreme precipitation conditions.

MATERIALS AND METHODS

Study area

Galería Los Elizondo is located within the metropolitan region of Monterrey in the state of Nuevo León, northeastern México. The area forms part of a semi-arid hydrological environment characterized by high interannual variability in precipitation and recurrent drought events that affect the availability of both surface and groundwater resources. Mean annual precipitation ranges between 500 and 700 mm, with rainfall concentrated primarily during short-duration convective storms occurring during the summer and early autumn months.

The study site is geographically referenced using Universal Transverse Mercator (UTM) coordinates X = 371,283.686 m and Y = 2,830,383.684 m, within a mountainous sector influenced by the structural geology of the Sierra Madre Oriental. The local relief is characterized by moderate slopes and carbonate lithologies typical of folded sedimentary sequences. Surface runoff occurs episodically during high-intensity precipitation events, generating concentrated flows along preferential drainage pathways controlled by the local terrain configuration (Eguiluz y de Antuñano and Chávez-Cabello, 2022).

The geographic location of the study area within the metropolitan region of Monterrey, northeastern México, together with its regional spatial context, is presented in Figure 1.

From a geological perspective, the region is dominated by carbonate formations composed primarily of limestone and dolomite, which have undergone extensive karstification through dissolution processes. The resulting subsurface structure contains fractures, bedding planes, conduits, and cavities that create a heterogeneous hydraulic medium. This structural complexity produces strong spatial variations in hydraulic conductivity and storage capacity within relatively short distances (Morán-Ramírez et al., 2018).

Hydrogeologically, the system corresponds to an unconfined karst aquifer influenced by local recharge processes and regional hydraulic gradients. Groundwater circulation is controlled by fracture networks and dissolution features that generate preferential flow paths and zones of enhanced permeability. The water table is relatively shallow in some sectors and deeper in others, reflecting the structural variability typical of karst systems.

The hydrological regime of the basin is strongly influenced by intense rainfall events associated with tropical storms and convective precipitation. These events generate rapid surface runoff that can be temporarily captured and directed toward infiltration systems. Such conditions make the area suitable for evaluating the feasibility of managed aquifer recharge through deep injection wells as a mechanism for enhancing groundwater storage under drought-prone climatic conditions.

The study was conceived as applied research aimed at the technical evaluation of an artificial recharge system through a deep injection well in a karst environment. It was developed as a single case study, considering Galería Los Elizondo as the unit of analysis, where the structural heterogeneity of the subsurface controls the hydraulic behavior of the aquifer.

The delineation of the area of influence was carried out through high precision topographic

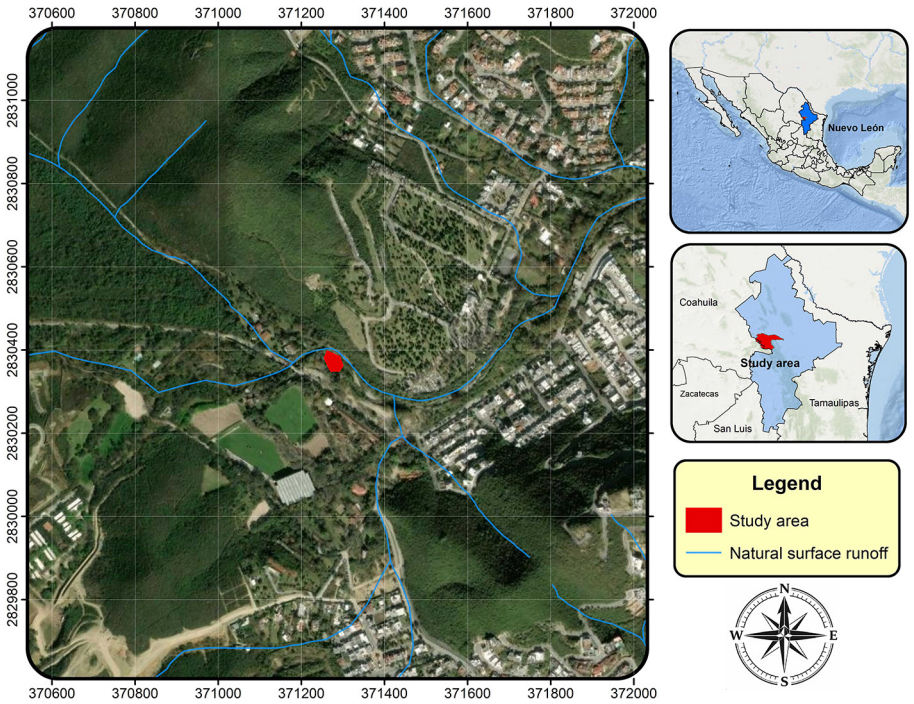

Figure 1. Geographic location of the Galería Los Elizondo study area within the metropolitan region of Monterrey, Nuevo León, northeastern México

surveying. Surface slopes, runoff pathways, and effective catchment area were defined. Based on these data, a digital elevation model was generated, allowing the establishment of the initial geometry of the system and the evaluation of surface drainage conditions. The site topography is presented in Figure 2.

For deep subsurface characterization, an exploratory sounding was executed to a depth of 800 m. This procedure made it possible to identify the stratigraphic sequence and estimate preliminary hydraulic parameters. In a complementary manner, magnetotelluric (MT) and transient electromagnetic time domain (TEM) studies were conducted. The records were processed through numerical inversion to obtain the distribution of resistivities as a function of depth, which made it possible to identify lithological contrasts and possible zones of greater hydraulic connectivity. The resistivity results obtained from the MT and TEM surveys are presented in Figure 3.

Hydrogeological characterization included the estimation of hydraulic conductivity and transmissivity by strata. Piezometric control points were installed and static levels were recorded over time to establish baseline conditions of the unconfined aquifer, as shown in Table 1 and Figure 4. In parallel, a preliminary hydrogeochemical analysis was conducted to verify compatibility between the recharge water and the receiving medium.

Within the hydrological component, pluviographic records from stations located near the site were compiled. The representative station was selected considering the distance to the basin centroid and the historical consistency of the record; subsequently, an analysis was carried out to obtain the discharges of the study basin. Figure 5 presents the results from the climatological station showing the maximum annual precipitation accumulated over 24 hours, in millimeters, for the study basin.

Extreme precipitation was analyzed using a GEV-MAX distribution with L-moments implemented in the Hydrognomon software. Table 2 shows the Kolmogorov–Smirnov test results, indicating that this distribution provides the best fit. Based on this probabilistic adjustment, height–duration–return period (HP-D-TR) and intensity–duration–return period (I-D-TR) curves were generated and used to define the rainfall intensity corresponding to the adopted return period in the hydraulic design (Courty et al., 2019), as shown in Figure 6 and Figure 7.

The HP–D–TR and I–D–TR curves were developed according to the proposals of Dick

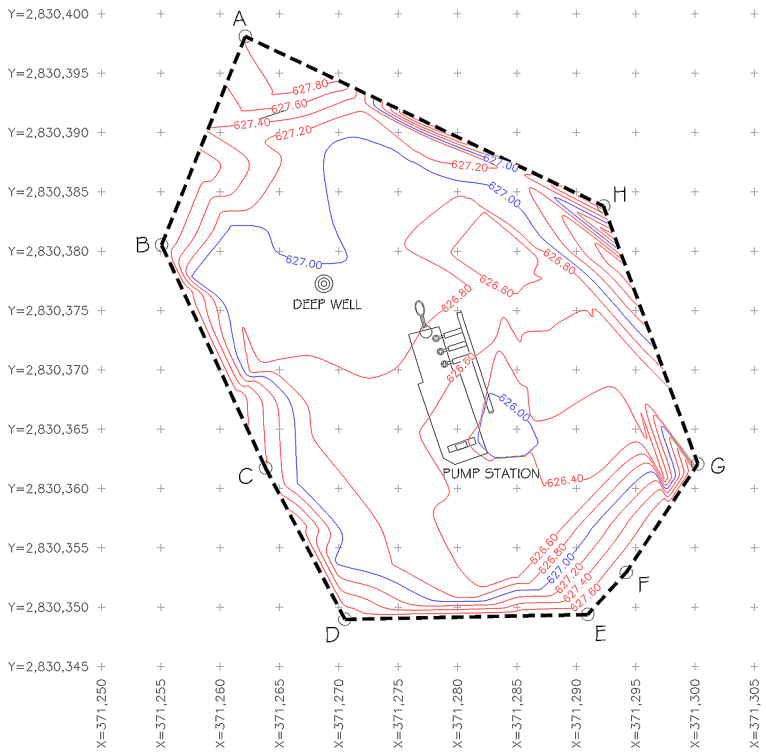

Figure 2. Site topography

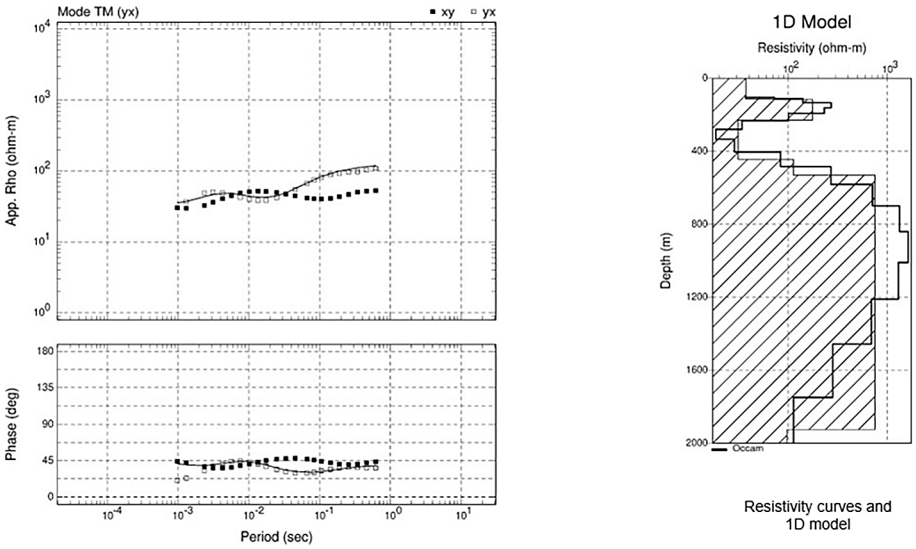

Figure 3. Electrical resistivity curves and 1D inversion model derived from MT and TEM surveys

Table 1. Location and elevation of monitoring wells (UTM coordinates)

Well	Easting (m)	Northing (m)	Elevation (masl)
P-1	371091.18	2830506.66	632
P-2	371294.04	2830376.64	626
P-3	371428.55	2830265.81	623
P-4	371640.34	2830348.12	616

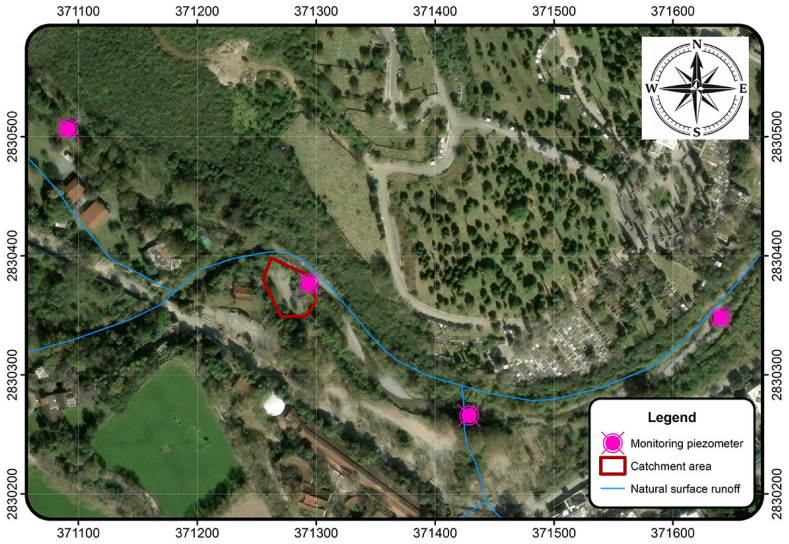

Figure 4. Location of monitoring wells

Peschke (Grundmann et al., 2019), which represent the rainfall depth–duration–return period and intensity–duration–return period relationships. It is important to note that this approach is suitable for rainfall durations of less than one hour. The equation used for its application is presented in Equation 1.

$$P_D = P_{24h} \times \left(\frac{d}{1440}\right)^{0.25} \quad (1)$$

where: Pd – total rainfall depth (mm), d – duration (min), $P24h$ – maximum 24-hour rainfall (mm), intensity is obtained by dividing the precipitation Pd by the duration.

The maximum design discharge was estimated using the Rational Method, integrating runoff coefficient, rainfall intensity, and effective catchment area. Based on this discharge, a hyetograph was constructed using the Alternating Block method with uniform temporal discretization, shown in

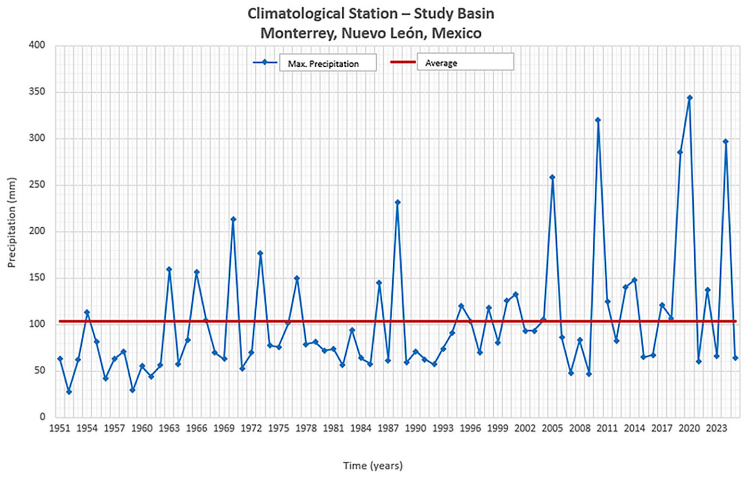

Figure 5. Maximum annual precipitation accumulated over 24 hours at the site

Table 2. Kolmogorov-Smirnov test results

Distribution	a=1%	a=5%	a=10%	Attained a	DMax
Normal	ACCEPT	REJECT	REJECT	1.10%	0.18627
Normal (L-moments)	REJECT	REJECT	REJECT	0.44%	0.20203
LogNormal	ACCEPT	ACCEPT	ACCEPT	26.59%	0.11591
Galton	ACCEPT	ACCEPT	ACCEPT	21.38%	0.12206
Exponential	ACCEPT	ACCEPT	ACCEPT	12.17%	0.1366
Exponential (L-moments)	ACCEPT	ACCEPT	ACCEPT	26.38%	0.11614
Gamma	ACCEPT	ACCEPT	REJECT	6.63%	0.1507
Pearson III	ACCEPT	ACCEPT	ACCEPT	12.34%	0.13626
Log Pearson III	ACCEPT	ACCEPT	ACCEPT	76.24%	0.07722
EV1-Max (Gumbel)	ACCEPT	ACCEPT	ACCEPT	12.11%	0.13672
EV2-Max	ACCEPT	ACCEPT	ACCEPT	12.63%	0.1357
EV1-Min (Gumbel)	REJECT	REJECT	REJECT	0.01%	0.25614
EV3-Min (Weibull)	ACCEPT	REJECT	REJECT	3.83%	0.16238
GEV-Max	ACCEPT	ACCEPT	ACCEPT	25.59%	0.11702
GEV-Min	ACCEPT	ACCEPT	ACCEPT	12.38%	0.13618
Pareto	ACCEPT	REJECT	REJECT	4.12%	0.16086
GEV-Max (L-moments)	ACCEPT	ACCEPT	ACCEPT	92.49%	0.06327
GEV-Min (L-moments)	ACCEPT	ACCEPT	ACCEPT	44.65%	0.0996
EV1-Max (Gumbel, L-moments)	ACCEPT	ACCEPT	REJECT	9.21%	0.14324
EV2-Max (L-moments)	ACCEPT	ACCEPT	ACCEPT	99.22%	0.04986
EV1-Min (Gumbel, L-moments)	REJECT	REJECT	REJECT	0.01%	0.26238
EV3-Min (Weibull, L-moments)	ACCEPT	ACCEPT	REJECT	8.93%	0.14973
Pareto (L-moments)	REJECT	REJECT	REJECT	-	0.41721
GEV-Max (kappa specified)	ACCEPT	ACCEPT	ACCEPT	38.70%	0.10441
GEV-Min (kappa specified)	REJECT	REJECT	REJECT	0.17%	0.21716
GEV-Max (kappa specified, L-moments)	ACCEPT	ACCEPT	ACCEPT	33.34%	0.10914
GEV-Min (kappa specified, L-moments)	REJECT	REJECT	REJECT	0.09%	0.22669

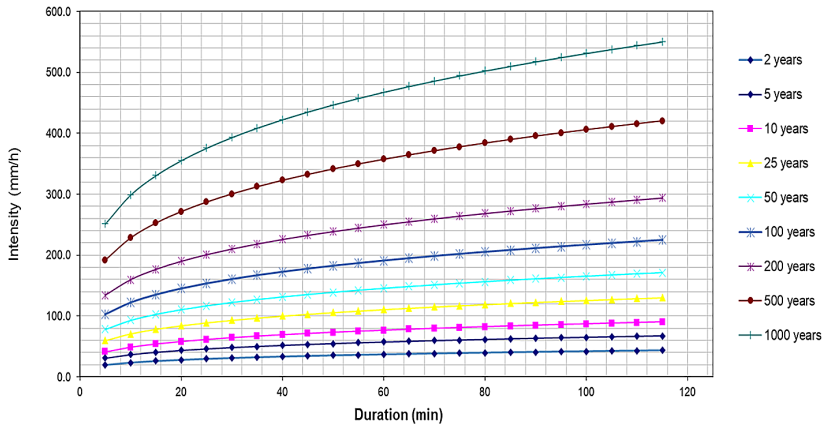

Figure 6. HP-D-TR curves

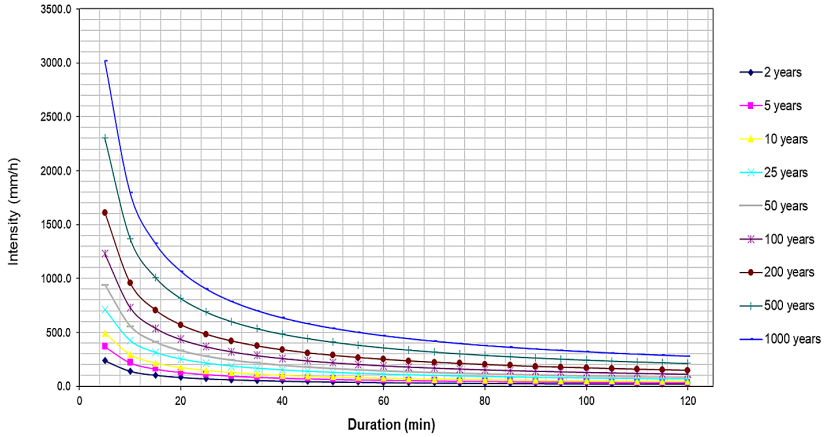

Figure 7. I-D-TR curves

Figure 8, from which the hydrograph was derived. Temporal integration made it possible to estimate the total volume associated with the design event.

The hydraulic sizing of the catchment system considered the calculation of the maximum head over the grate, the determination of the required effective area, and the conveyance capacity using the Manning equation for gravity flow. The pipe diameter was selected according to the estimated maximum discharge and the anticipated operating conditions.

From a geotechnical perspective, the physical and mechanical properties of the ground were evaluated to ensure the structural stability of the well and its associated components. Support conditions and soil behavior under drilling and infiltration processes were analyzed.

The structural design of the well included internal diameter, effective depth, and the selection of materials compatible with the aquifer chemistry. A safety factor was incorporated in the estimation of the effective internal area, and the hydraulically active length and effective transient storage volume were determined.

Hydraulic performance verification was carried out through a volume–time balance discretized into uniform intervals. A cumulative table of inflow volumes, infiltrated volumes, and associated times was prepared to identify the point of maximum system demand. Piezometric records were evaluated using analysis of variance (ANOVA) in order to verify the statistical consistency of the observed behavior.

Field implementation

Experimental methods were oriented toward controlled technical procedures suitable for drilling recharge wells in deep aquifers located within heterogeneous karst environments. In the construction of recharge wells for groundwater systems, drilling techniques must be adapted to site conditions in order to ensure operational stability and long-term functionality of the system.

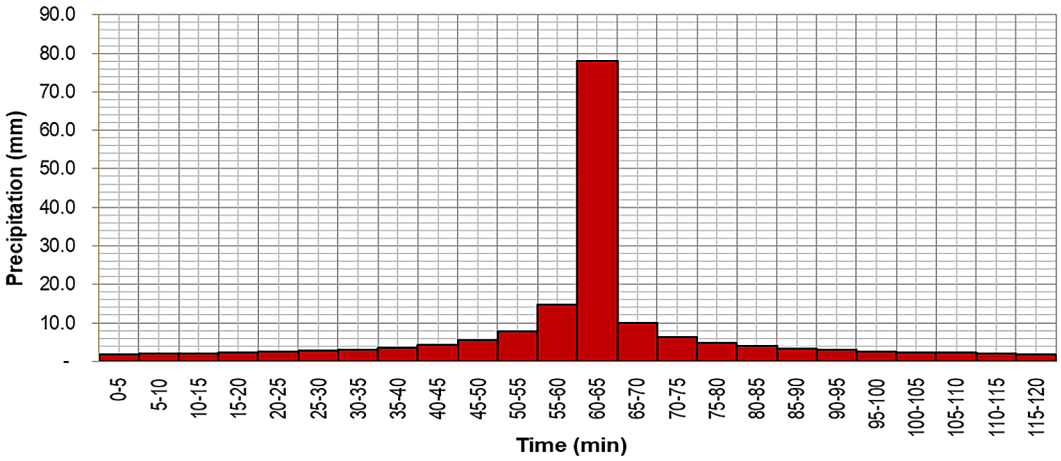

Figure 8. Hyetograph by the alternating block method

For drilling operations, a rotary drilling method was applied, in which drill bits rotate continuously and progressively penetrate the ground. This drilling technique allows the controlled advancement of the borehole while enabling the removal of material and the recovery of lithological samples as depth increases. Rotary drilling is commonly employed in groundwater exploration because it allows effective penetration through fractured carbonate formations typical of karst environments.

During the drilling process, obstructions encountered within the subsurface were removed through mechanical means that facilitate excavation and maintain drilling continuity. The sounding was carried out progressively in stages, following procedures designed to prevent structural instability, particularly in fractured zones or sectors where the geological material presents variable mechanical resistance.

Well stability depends on maintaining controlled drilling progression and ensuring that borehole walls remain structurally stable during advancement. The rate of drilling progress and the final depth reached depend primarily on the lithological characteristics of the carbonate formations encountered and the structural conditions present in the subsurface.

Throughout the drilling process, geological material obtained during advancement was examined in order to verify the stratigraphic interpretation previously inferred from geophysical surveys. Continuous monitoring of borehole conditions and drilling progression was carried out to ensure operational safety and to guarantee the technical feasibility of the recharge well installation within the karst aquifer system.

Once drilling reached the required depth, the borehole was conditioned to allow the installation of the recharge well components and to ensure adequate hydraulic interaction with the receiving aquifer. These procedures included the stabilization of the borehole walls and the preparation of the internal structure necessary for the operation of the recharge system under the hydrogeological conditions identified during the site characterization stage.

Instrumentation

The equipment used in this study included drilling machinery, surveying instruments, and computer software required for fieldwork, data acquisition, and technical design. The deep injection well was drilled using a B-50 mobile drilling rig, which is suitable for operation in areas with difficult access and under variable subsurface conditions, while allowing geological samples to be recovered as drilling progresses.

Georeferencing of the study area and acquisition of spatial data were carried out using a Magellan Promark 3 GPS receiver with a dual GPS receiver and integrated antenna, enabling the collection of high-precision coordinates for topographic surveying and site delineation. Topographic measurements were performed with a Nikon DTM-322 electronic distance measurement (EDM) total station, which allows distance measurements of up to 2,000 m with a prism, records horizontal and vertical angles in accordance with DIN 18723 standards, and stores up to 25,000 points. Data can be transferred through an RS-232C connection or by wireless communication.

Computer software was used for technical drafting, data processing, and report preparation. AutoCAD was employed to produce two-dimensional drawings and technical representations required for the design of the deep injection system. Microsoft Office was used for document preparation, data processing, and the organization of project-related reports. Hydrological data processing and analysis were conducted using Hydrognomon, which supports time-series management and calculations related to water balance and rainfall analysis.

RESULTS

The system was defined at the UTM coordinates X = 371,283.686 m and Y = 2,830,383.684 m, integrating with the existing infrastructure within the study area. The effective catchment area was established as a 15 × 30 m rectangle, equivalent to 450 m² (0.045 ha), with a 1% surface slope to ensure gravitational runoff toward the conveyance system as shown in Figure 9.

Electrical resistivity measurements obtained through magnetotelluric (MT) and transient electromagnetic (TEM) methods ranged from 23 to 270 Ω·m within the first few hundred meters, and resistivities close to 1,000 Ω·m at approximate depths of 600 m. These results confirm the structural heterogeneity of the carbonate medium and support the adopted hydraulic stratification (Díaz-Bravo et al., 2022).

The hydrogeological characterization allowed the definition of differentiated hydraulic conductivity and thickness parameters. For the shallow aquifer, two units were considered (b = 20 m, K = 100 m/day; b = 90 m, K = 10 m/day). For the deep aquifer, four strata were adopted (b = 20 m, K = 10 m/day; b = 30 m, K = 10 m/day; b = 100 m, K = 10 m/day; b = 55 m, K = 0.1 m/day).

The piezometric monitoring conducted at points P-1, P-2, P-3, and P-4 recorded groundwater elevations of 625.167, 625.017, 620.946, and 612.897 masl, respectively, resulting in an overall average elevation of 621.007 masl. The results are shown in Table 3.

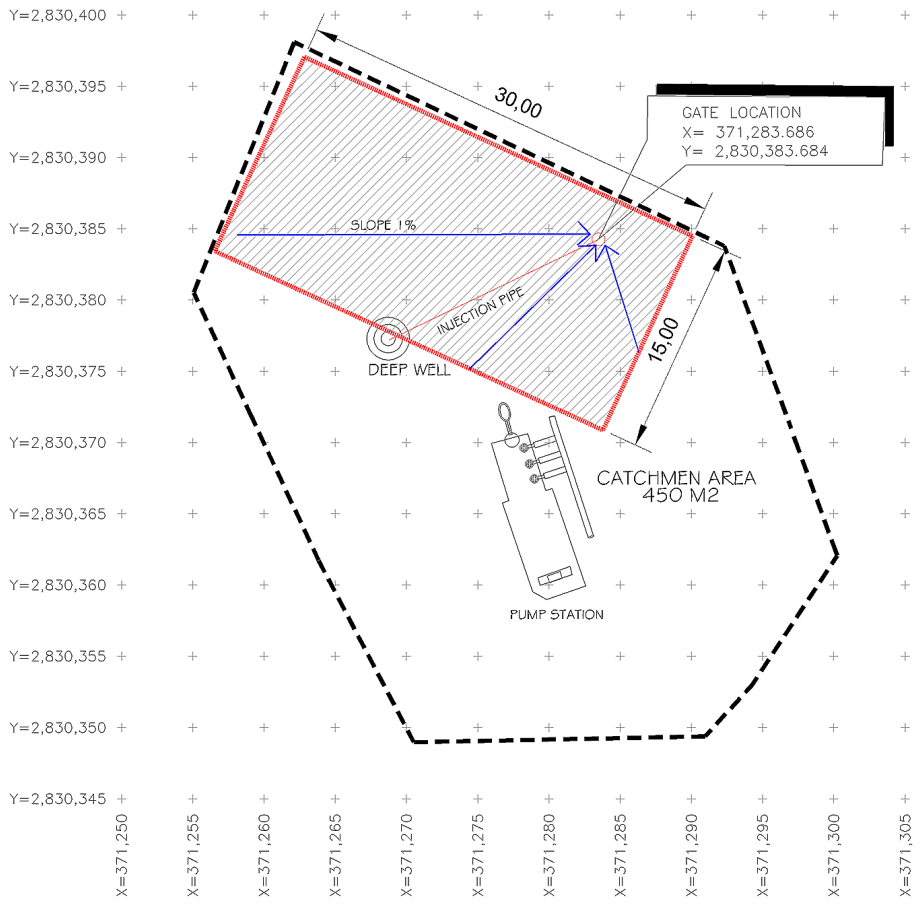

Figure 9. Location of the precipitation recharge well

Considering a wellhead elevation of approximately 628 masl, the average depth to the shallow water table was approximately 6.99 m, obtained as the difference between the ground surface elevation and the mean piezometric level.

ANOVA shown in Tables 4, 5, and 6 revealed highly significant differences among the recorded groundwater levels ($F = 8967.97$; $p < 0.001$; $\alpha = 0.05$), with an adjusted coefficient of determination of $R^2 = 99.66\%$ (Table 6). These results indicate that the observed variability is primarily associated with systematic differences among the monitoring points rather than random variation. The high R^2 value confirms the strong explanatory capacity of the statistical model and reflects the spatial differentiation of groundwater levels within the monitored aquifer system (Kim, 2017).

Tukey's multiple comparison test (Montgomery, 2019) showed that P-1 and P-2 belong to the same statistical group, whereas P-3 and P-4 exhibit significantly greater declines (Table 7).

Temporal analysis using polynomial regression revealed statistically significant behavior at monitoring points P-1 ($F = 122.95$; $p < 0.001$; $R^2 = 92.48\%$), P-2 ($F = 53.73$; $p < 0.001$; $R^2 = 84.31\%$), P-3 ($F = 4.27$; $p = 0.028$; $R^2 = 29.94\%$), and P-4 ($F = 17.30$; $p < 0.001$; $R^2 = 63.37\%$), as presented in Table 8 and Figure 10.

For a 50-year return period event, application of the rational method ($C = 0.90$; $I = 937.05$ mm/h; duration = 5 min) resulted in an estimated peak discharge of 105 L/s. The rainfall intensity was derived from the intensity–duration–return period (I–D–TR) curve obtained from the extreme rainfall analysis. The equation used to calculate the maximum discharge is presented below in Equation 2.

$$Q_{max} = 0.00278\, C\, I\, A \tag{2}$$

where: Q_{max} – maximum design discharge (m^3/s), C – runoff coefficient (dimensionless), I – rainfall intensity (mm/h), A – contributing drainage area (ha), and 0.00278 – conversion factor that ensures dimensional consistency in the International System of Units (SI).

Table 3. Monitoring well measurements

Piezometric level (masl)				
Date	P-1	P-2	P-3	P-4
02/08/2021	625.32	625.21	621.33	613.74
06/09/2021	625.29	625.20	621.33	613.72
04/10/2021	625.30	625.16	621.36	613.78
01/11/2021	625.24	625.08	621.32	613.52
06/12/2021	625.22	625.04	621.13	613.31
03/01/2022	625.21	625.03	620.80	612.98
07/02/2022	625.23	625.06	620.75	612.92
07/03/2022	625.20	625.07	620.58	612.76
04/04/2022	625.18	625.08	620.55	612.63
02/05/2022	625.19	625.09	620.66	612.84
06/06/2022	625.17	625.07	620.78	612.97
04/07/2022	625.12	625.06	620.85	612.48
01/08/2022	625.13	625.02	620.90	612.95
05/09/2022	625.11	624.96	621.05	613.20
03/10/2022	625.12	624.95	621.18	613.07
07/11/2022	625.09	624.92	621.22	613.02
05/12/2022	625.08	624.90	621.10	612.52
02/01/2023	625.08	624.89	620.85	612.42
06/02/2023	625.07	624.90	620.80	611.97
06/03/2023	625.09	624.92	620.76	612.02
03/04/2023	625.12	624.93	620.73	612.19
01/05/2023	625.13	624.91	620.78	612.65
05/06/2023	625.15	624.93	620.95	612.98

Table 4. Factor information

Factor	Levels	Values
Monitoring point	4	P-1, P-2, P-3, P-4

Substituting the design parameters into Equation 2 yields:

$$Q_{max} = 0.00278 \cdot 0.9 \cdot 937.05 \cdot 0.045$$
$$Q_{max} = 105\ L/s \quad (3)$$

The runoff response of the basin was represented through the unit hydrograph derived from the design storm event. This hydrograph characterizes the temporal distribution of surface runoff generated within the contributing drainage area and provides an estimate of the dynamic response of the basin to intense precipitation. The shape of the hydrograph reflects the concentration of runoff toward the outlet, where the rising limb corresponds to the rapid accumulation of flow generated by the rainfall excess. The peak discharge reached approximately 105 L/s, occurring shortly after the time to peak estimated for the basin. Following the peak, the recession limb shows the progressive reduction in discharge as infiltration and storage processes within the basin attenuate the flow. The resulting hydrograph describing the temporal evolution of discharge during the design storm event is presented in Figure 11.

The hydraulic design of the intake structure resulted in a maximum flow depth of 0.142 m and a required effective inlet area of 0.299 m², which was resolved using a 0.50 m² grate module.

Conveyance toward the injection well was designed under gravity flow conditions using the Manning equation (Chanson, 2014), selecting a commercial pipe diameter of 14 inches.

The injection well was defined with an internal diameter of 24 inches and an approximately 400 m hydraulically active length, providing an effective temporary storage volume of 40.58 m³. A schematic representation of the proposed

Table 5. Analysis of variance

Source	GL	SC adjusted	MC adjusted	F value	P value
Factor	3	2280.47	760.157	8967.97	< 0.001
Error	88	7.46	0.085		
Total	91	2287.93			

Table 6. Model summary

S	R-square	R-square adjusted	R-square pred.
0.291142	99.67%	99.66%	99.64%

Table 7. Tukey's comparison

Factor	N	Average	Grouping		
P-1	23	625.167	A		
P-2	23	625.017	A		
P-3	23	620.946		B	
P-4	23	612.897			C

Table 8. R-square results

Factor	S	R-square	R-square adjusted
P-1	0.0213576	92.48%	91.73%
P-2	0.0406993	84.31%	82.74%
P-3	0.222628	29.94%	22.94%
P-4	0.323443	63.37%	59.71%

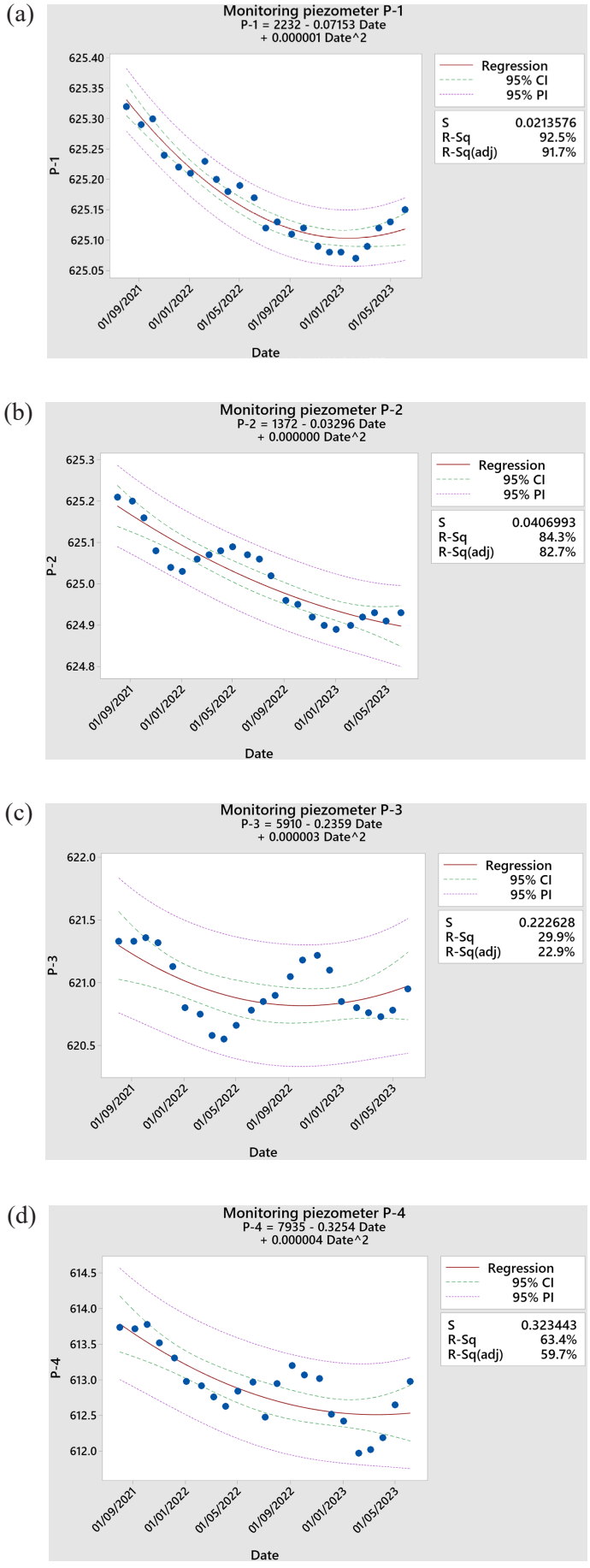

Figure 10. Temporal regression analysis of groundwater levels at monitoring points: (a) P-1, (b) P-2, (c) P-3, (d) P-4

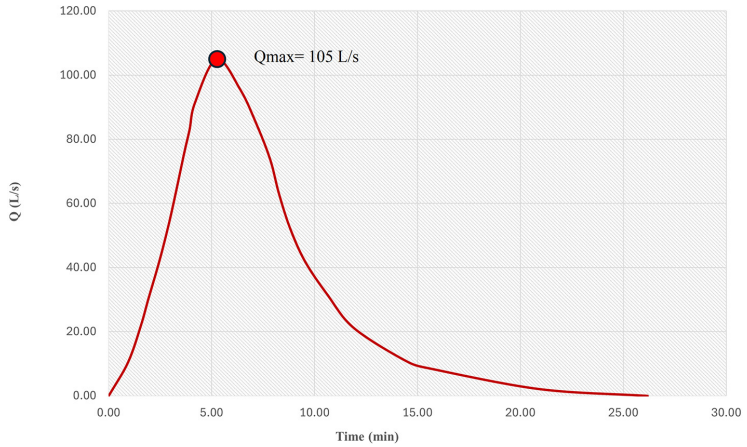

Figure 11. Unit hydrograph obtained for the study basin showing the temporal evolution of discharge during the design storm event (Qmax ≈ 105 L/s)

recharge well supplied by stormwater runoff is presented below in Figure 12 and Figure 13.

The volume–time analysis discretized into 5-minute intervals identified a minimum storage margin of −4.51 m³ around minutes 25–35 of the design storm event, indicating that the cumulative inflow temporarily exceeded the effective storage capacity of the well during a single interval. Subsequently, the system recovered storage capacity as the hydrological input decreased and infiltration into the aquifer continued. The infiltration capacity of the system was estimated from the hydraulic response observed during the volume–time balance of the design storm event. Considering the effective storage volume of the well and the hydraulic response during the infiltration process, an equivalent infiltration rate of approximately 125.539 mm/h was obtained. This value represents the hydraulic dissipation capacity of the system toward the aquifer through the direct interaction between the well structure and the fractured carbonate formations present in the study area. Such infiltration rates are consistent with the hydraulic behavior commonly observed in karst aquifers, where fractures, dissolution conduits, and preferential flow paths significantly

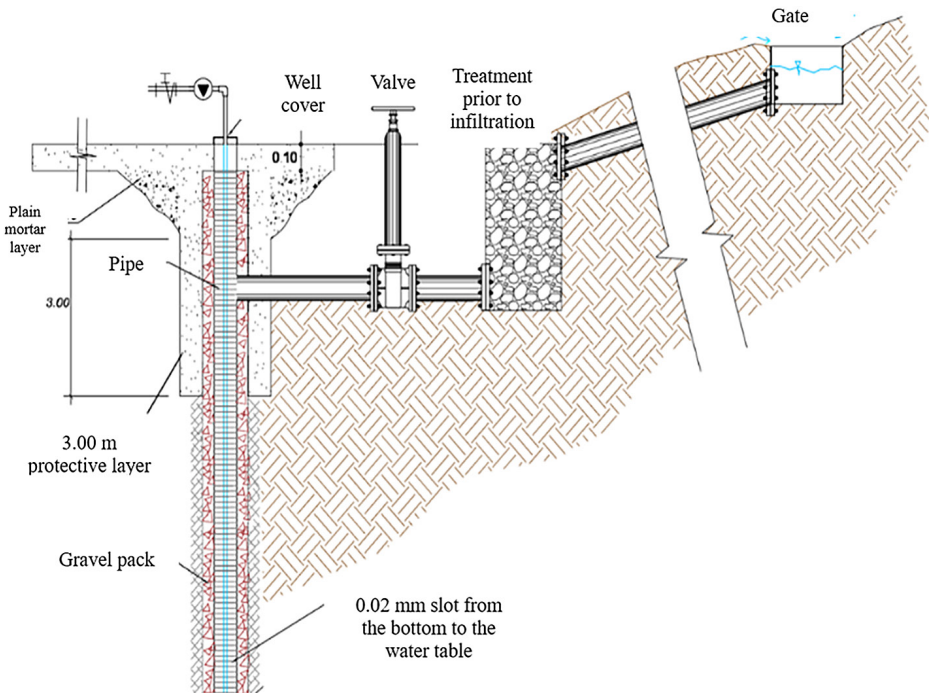

Figure 12. Schematic representation of the proposed recharge well supplied by stormwater runoff

Figure 13. Surface structure of the recharge well used for stormwater injection at the Galería Los Elizondo site

enhance groundwater infiltration compared with porous media aquifers. The results are presented below in Table 9.

DISCUSSION

The geophysical characterization of the subsurface using magnetotelluric (MT) and transient electromagnetic (TEM) methods identified resistivity contrasts ranging from 23 to 270 Ω·m within the first few hundred meters, and values approaching 1000 Ω·m at greater depths. This distribution confirms the structural heterogeneity of the carbonate medium and supports the hydraulic stratification adopted in the conceptual model. In karst environments, where secondary porosity and hydraulic anisotropy govern effective transmissivity, the integration of geophysical data reduces uncertainty associated with subsurface flow behavior and prevents the assumption of medium homogeneity (Stevanović, 2019).

From a hydrogeological perspective, the differentiated hydraulic conductivity parameters assigned to individual strata indicate a system composed of highly connected units superimposed over sectors of lower transmissivity. This configuration explains the spatial variability observed in piezometric levels and is consistent with the statistical results obtained from the ANOVA, which revealed significant differences among monitoring points. Polynomial regression analyses confirmed differentiated temporal trends, consistent with an unconfined aquifer influenced by climatic variability and local hydraulic gradients.

Within the hydrological component, the 50-year return period design event generated an estimated total runoff volume of 370.41 m³. The effective temporary storage capacity of the injection well was calculated at 40.58 m³, establishing a structurally asymmetric relationship between inflow volume and instantaneous storage capacity. This relationship demonstrates that the system was not conceived as a reservoir intended to fully retain the extreme event volume, but rather as a temporary hydraulic attenuation mechanism whose performance depends on progressive infiltration into the aquifer (Maliva, 2020).

The discretized volume–time balance using 5-minute intervals identified a minimum volumetric margin of −4.51 m³ during the peak concentration segment of the hydrograph, indicating a transient exceedance of effective capacity within a single critical interval. This behavior is characteristic of capture and injection systems in which surface storage acts as a regulating volume while infiltration progressively compensates for the excess inflow. The subsequent system recovery confirms that the infiltration rate is sufficient to restore hydraulic equilibrium once the event peak has passed.

The difference between the extreme event volume and the system's effective storage

Table 9. Results of stormwater recharge filling time analysis

Time	Interval	Precipitation	Intensity	Infiltration	Va	Vi	Va cumulative	Vi cumulative	Va cumulative - Vi cumulative	Margin
min	min	mm	mm/hr	mm/hr	m³	m³	m³	m³	m³	m³
0	0	0.000	0.000	125.539	0.000	0.000	0.000	0.000	0.000	40.585
5	5	78.088	937.053	125.539	31.626	8.016	31.626	8.016	23.610	16.975
10	5	92.862	557.175	125.539	18.805	8.016	50.430	16.031	34.399	6.186
15	5	102.769	411.077	125.539	13.874	8.016	64.304	24.047	40.257	0.328
20	5	110.433	331.298	125.539	11.181	8.016	75.485	32.062	43.423	-2.838
25	5	116.768	280.244	125.539	9.458	8.016	84.944	40.078	44.866	-4.281
30	5	122.214	244.428	125.539	8.249	8.016	93.193	48.094	45.099	-4.514
35	5	127.016	217.741	125.539	7.349	8.016	100.542	56.109	44.433	-3.848
40	5	131.327	196.991	125.539	6.648	8.016	107.190	64.125	43.065	-2.480
45	5	135.252	180.336	125.539	6.086	8.016	113.277	72.140	41.136	-0.551
50	5	138.862	166.634	125.539	5.624	8.016	118.900	80.156	38.744	1.841
55	5	142.210	155.138	125.539	5.236	8.016	124.136	88.172	35.965	4.620
60	5	145.338	145.338	125.539	4.905	8.016	129.042	96.187	32.854	7.731
65	5	148.275	136.869	125.539	4.619	8.016	133.661	104.203	29.458	11.127
70	5	151.048	129.470	125.539	4.370	8.016	138.030	112.218	25.812	14.773
75	5	153.676	122.941	125.539	4.149	8.016	142.180	120.234	21.946	18.639
80	5	156.175	117.132	125.539	3.953	8.016	146.133	128.250	17.883	22.702
85	5	158.560	111.925	125.539	3.777	8.016	149.910	136.265	13.645	26.940
90	5	160.843	107.228	125.539	3.619	8.016	153.529	144.281	9.249	31.336
95	5	163.031	102.967	125.539	3.475	8.016	157.004	152.296	4.708	35.877
100	5	165.135	99.081	125.539	3.344	8.016	160.348	160.312	0.036	40.549
105	5	167.162	95.521	125.539	3.224	8.016	163.572	168.328	-4.755	45.340
110	5	169.117	92.246	125.539	3.113	8.016	166.686	176.343	-9.658	50.243
115	5	171.007	89.221	125.539	3.011	8.016	169.697	184.359	-14.662	55.247
120	5	172.837	86.418	125.539	2.917	8.016	172.613	192.374	-19.761	60.346

capacity indicates that approximately 89% of the inflow does not rely on static storage. Instead, system behavior depends primarily on infiltration dynamics during hydrograph development. Consequently, system performance depends primarily on the transmission capacity of the receiving medium rather than on well geometry alone (Pyne, 2014). This behavior highlights the importance of integrating geophysical characterization, extreme rainfall hydrological analysis, and discretized volume–time verification in the evaluation of recharge systems in heterogeneous karst aquifers. The sequential combination of topographic analysis, geophysical exploration, hydrogeological characterization, hydrological modeling, and hydraulic verification provides a coherent methodological framework for assessing the technical performance of managed aquifer recharge systems under complex geological conditions.

In heterogeneous karst environments, where fractures and preferential conduits may significantly alter hydraulic response, discretized volumetric control constitutes a fundamental verification criterion. The explicit identification of the critical interval and maximum demand margin enables quantification of the operational threshold under extreme conditions and provides an objective parameter for evaluating additional safety factors or potential design adjustments.

Overall, the results demonstrate that integrating geophysical characterization, extreme-event hydrological analysis, and discretized volume–time verification allows system behavior to be interpreted consistently with the structural nature of the aquifer. The adopted model incorporates subsurface heterogeneity within a quantitatively verifiable framework that defines operational limits, temporal response, and attenuation capacity under design conditions.

CONCLUSIONS

The integration of geophysical, hydrogeological, hydrological, and hydraulic information enabled a quantitative characterization of the deep injection recharge system operating within a heterogeneous karst environment. Resistivity contrasts obtained through magnetotelluric and transient electromagnetic methods revealed a stratified structure with significant variations in connectivity and transmissivity, consistent with the differentiated hydraulic behavior observed in piezometric monitoring.

Statistical analysis confirmed the presence of significant differences among groundwater levels recorded at the monitoring points. The ANOVA yielded significance values below 0.05, while Tukey's multiple comparisons identified distinct groupings, indicating a spatially non-uniform response within the shallow aquifer. Polynomial regression models revealed temporal trends consistent with regional hydrological variability.

The hydrological scenario corresponding to a 50-year return period event produced a total runoff volume of 370.41 m³, derived from application of the rational method and hydrograph construction using the alternating block method. The effective well storage volume was quantified at 40.58 m³, and the discretized 5-minute volume–time analysis identified a transient volumetric exceedance during a single critical interval, with a maximum deficit of −4.51 m³ at peak hydrograph concentration.

This behavior indicates that, under the extreme design event considered, the system experiences a momentary volumetric exceedance that is subsequently compensated by progressive infiltration into the aquifer. The estimated filling time ranged between 15 and 45 minutes, reflecting a transient storage dynamic with a reduced operational margin under maximum precipitation conditions.

The findings indicate that system evaluation must adopt an integrated framework incorporating structural characterization of the receiving medium, extreme-event hydrological analysis, and discretized volumetric verification. Explicit identification of the maximum hydraulic demand point provides a technical basis for adjusting safety factors, optimizing design parameters, or implementing flow control strategies under future operational scenarios. This methodological framework may serve as a practical reference for the technical design and evaluation of managed aquifer recharge systems in heterogeneous karst environments subject to extreme hydrological variability.

Acknowledgements

The authors would like to express their sincere gratitude to the Universidad Autónoma de Nuevo León and the Faculty of Civil Engineering for their institutional support and for providing the academic environment and resources necessary for the development of this research.

REFERENCES

1. Binley, A., Hubbard, S. S., Huisman, J. A., Revil, A., Robinson, D. A., Singha, K., Slater, L. D. (2015). The emergence of hydrogeophysics for improved understanding of subsurface processes over multiple scales. *Water Resources Research, 51*(6), 3837–3866. https://doi.org/10.1002/2015WR017016
2. Chanson, H. (2014). *Hydraulics of open channel flow* (2nd ed.). Butterworth-Heinemann. https://doi.org/10.1016/B978-0-7506-5978-9.X5000-4
3. Courty, L. G., Wilby, R. L., Hillier, J. K. (2019). Intensity–duration–frequency curves at the global scale. *Environmental Research Letters, 14*(8), 084045. https://doi.org/10.1088/1748-9326/ab370a
4. Cristiano, E., ten Veldhuis, M.-C., van de Giesen, N. (2017). Spatial and temporal variability of rainfall and their effects on hydrological response in urban areas: A review. *Hydrology and Earth System Sciences, 21*, 3859–3878. https://doi.org/10.5194/hess-21-3859-2017
5. Cruz-Ayala, M. B., Megdal, S. B. (2020). An overview of managed aquifer recharge in México and its legal framework. *Water, 12*(2), 474. https://doi.org/10.3390/w12020474
6. Díaz-Bravo, B. A., Ortega-Obregón, C., Barboza-Gudiño, J. R. (2022). U–Pb geochronology of intrusive rocks of northwestern Mesa Central province and the transversal sector of the Sierra Madre Oriental, México: Time and space distribution of inland Cretaceous–Paleogene magmatism during the Mexican orogeny. *Journal of South American Earth Sciences, 117*, 103989. https://doi.org/10.1016/j.jsames.2022.103989
7. Eguiluz y de Antuñano, S., Chávez-Cabello, G. (2022). Extensión sinsedimentaria del Cretácico Inferior en el borde del Bloque Coahuila, un margen tipo rift en México. *Boletín de la Sociedad Geológica Mexicana, 74*(1), A130821. https://doi.org/10.18268/BSGM2022v74n1a130821

8. Famiglietti, J. S. (2014). The global groundwater crisis. *Nature Climate Change, 4*(11), 945–948. https://doi.org/10.1038/nclimate2425
9. Goldscheider, N., Chen, Z., Auler, A. S., Bakalowicz, M., Broda, S., Drew, D., Hartmann, J., Jiang, G., Moosdorf, N., Stevanović, Z., Veni, G. (2020). Global distribution of carbonate rocks and karst water resources. *Hydrogeology Journal, 28*, 1661–1677. https://doi.org/10.1007/s10040-020-02139-5
10. Grundmann, J., Bronstert, A., Bárdossy, A. (2019). Stochastic reconstruction of spatio-temporal rainfall patterns for hydrological modelling. *Hydrology and Earth System Sciences, 23*, 225–237. https://doi.org/10.5194/hess-23-225-2019
11. Hartmann, A., Goldscheider, N., Wagener, T., Lange, J., Weiler, M. (2014). Karst water resources in a changing world: Review of hydrological modeling approaches. *Reviews of Geophysics, 52*(3), 218–242. https://doi.org/10.1002/2013RG000443
12. Kim, T. K. (2017). Understanding one-way ANOVA using conceptual figures. *Korean Journal of Anesthesiology, 70*(1), 22–26. https://doi.org/10.4097/kjae.2017.70.1.22
13. Maliva, R. G. (2020). *Anthropogenic aquifer recharge*. Springer. https://doi.org/10.1007/978-3-030-11084-0
14. Montgomery, D. C. (2019). *Design and analysis of experiments* (10th ed.). John Wiley & Sons.
15. Morán-Ramírez, J., Ramos-Leal, J. A., Mahlknecht, J., Santacruz-De León, G., Martín-Romero, F. (2018). Modeling of groundwater processes in a karstic aquifer of the Sierra Madre Oriental, México. *Applied Geochemistry, 97*, 41–56. https://doi.org/10.1016/j.apgeochem.2018.05.011
16. Neri, C., Magaña, V. (2016). Estimation of vulnerability and risk to meteorological drought in México. *Weather, Climate, and Society, 8*(2), 95–110. https://doi.org/10.1175/WCAS-D-15-0005.1
17. Palma, A., Rivera, A., Carmona, R. (2022). A unified hydrogeological conceptual model of the México Basin Aquifer after a century of groundwater exploitation. *Water, 14*(10), 1584. https://doi.org/10.3390/w14101584
18. Pyne, R. D. (2014). *Groundwater recharge and wells: A guide to aquifer storage recovery*. CRC Press.
19. Stefan, C., Ansems, N. (2018). Web-based global inventory of managed aquifer recharge applications. *Sustainable Water Resources Management, 4*, 153–162. https://doi.org/10.1007/s40899-017-0212-6
20. Stevanović, Z. (2019). Karst waters in potable water supply: A global scale overview. *Environmental Earth Sciences, 78*, 662. https://doi.org/10.1007/s12665-019-8670-9